Available online at www.sciencedirect.com
ScienceDirect
Trans. Nonferrous Met. Soc. China 23(2013) 3286−3292
Transactions of Nonferrous Metals Society of China
www.tnmsc.cn

Growth and crystallization behaviors of anodic oxide films on sputter-deposited titanium at very low potentials

Jun-heng XING, Zheng-bin XIA, Hui LI, Ying-ying WANG, Li ZHONG
School of Chemistry and Chemical Engineering, South China University of Technology, Guangzhou 510640, China

Received 11 December 2012; accepted 30 January 2013

Abstract: Growth and crystallization of titanium anodized films were studied by performing the anodization of the sputter-deposited titanium samples under cyclic voltammetry (CV) mode at very low potentials. The surface features, crystalline behaviors and chemical compositions of the formed anodic oxide layers were detected by AFM, SE and XPS. It was found that the structure of the titanium anodized films is crystalline, even though the maximum oxidation potential (φ_{max}) is very low (as low as 1000 mV). Both enlarging the applied voltage and reducing the potential scanning rate are beneficial for the growth and crystallization of titanium oxide films. It was thought that the internal compressive stress, other than the local joule heating accepted for many researchers, is the main force of stimulating the crystallization of anodic titanium oxide films at very low potentials.
Key words: anodization; sputter-deposited titanium; crystallization; low potential; cyclic voltammetry (CV)

1 Introduction

Titanium oxide thin films prepared by electrochemical anodization methods have been widely studied for their potential use in areas of sensors, solar cells, photocatalytic engineering and biomedical engineering, etc [1−6]. The application performance of titanium anodized films is determined by their structure and surface features [7,8]. It is generally accepted that the titanium oxide layers will grow with crystalline structure only when the applied voltages are high enough [6,9−11]. For example, by Raman spectroscopy, SI et al [10] revealed that the titanium oxide film formed below 40 V was amorphous.

However, in some other studies, the titanium oxide thin films were proved to have crystalline structure, even though the oxidation potential was very low [12]. It was reported that the anodic oxide layers grown at low potentials were very thin and their crystalline structure was short-range order instead of long-range order [13,14]. Hence, the traditional characterization methods for detection of crystalline TiO_2, such as X-ray diffraction (XRD) and Raman spectra, are not suitable for the oxide films grown at very low potentials. In fact, as revealed by some authors, the atoms in the titanium oxide film have been rearranged towards a more ordered structure, even before crystalline forms were detected [15]. By X-ray absorption spectroscopy (XAS), FONSECA et al [14] revealed that a short-range order structure existed in the titanium oxide film, even though the film structure appeared to be amorphous by grazing X-ray diffraction (GXRD). Similarly, as reported by HABAZAKI et al [16], short-range ordered oxides of sub-nm size were generated on the film surface in the initial stage of titanium anodization, and subsequently, these relatively ordered oxides would act as crystal nucleuses and grow up to large crystalline grains with the time prolonging.

In the present work, we fabricated thin anodic oxide films on atomically flat sputter-deposited titanium samples at very low potentials, so that the evolution of the structure and surface features of titanium oxide films during the anodization process could be studied from a microcosmic view. For the purpose that the growth and crystallization of the oxide films would go through a very slow process, the cyclic voltammetry (CV) technique was used for the titanium anodization.

2 Experimental

Titanium thin films with atomically flat surface were deposited onto monocrystal silicon substrates by

Foundation item: Project (20976058) supported by the National Natural Science Foundation of China
Corresponding author: Zheng-bin XIA; Tel: +86-20-87112047; Fax: +86-20-87112093; E-mail: cezhbxia@scut.edu.cn
DOI: 10.1016/S1003-6326(13)62865-4

magnetron sputtering method. The root mean square roughness (R_{ms}) of the samples surface was less than 0.5 nm. Subsequently, the samples were diced into small sheet with dimensions of 8 mm×10 mm and used as the working electrode. Anodizing of titanium was carried out in a three-electrode electrochemical cell set-up with a Pt counter electrode, and a saturated Ag/AgCl reference electrode (to which all potentials were referred in this work). An Autolab PGSTAT100 electrochemical workstation (Metrohm, Switzerland) was used to maintain the anodization procedure. The electrolyte was 0.1 mol/L H_2SO_4 solution, and all experiments were carried out at 25 °C. Before anodization, all samples were cathodically treated as described in Ref. [13]. The CV mode was used for the film growth. The potential scan started at −280 mV and ended with different maximum oxidation potential (φ_{max}), the cycle number was five, and the potential sweep rates were 0.05, 0.1 or 0.5 mV/s, respectively.

The surface topography of titanium anodized films was detected by atomic force microscopy (AFM, BENYUAN CSPM 4000, China) using a tapping mode. The root mean square roughness and average roughness (R_a) of the anodized samples were obtained from the AFM results by the accompanied IMAGE 4.60 software. Spectroscopic ellipsometer (SE, HORIBA Jobin Yvon Auto SE, France) was used to determine the thickness and optical properties of titanium oxide films. The measurements were performed at an incidence angel of 70° in the wavelength range of 439−842 nm. A two-layer model (Si/Ti/TiO_2) was used in the modeling procedure. X-ray photoelectron spectrometry (XPS, Kratos Axis Ultra DLD, UK), which was performed using an Al K_α (1486.6 eV) X-ray source operated at 15 kV and 150 W, was used to detect the chemical composition of the anodized films. The spectral positions were corrected by normalizing the C 1s spectrum at 284.6 eV, and a Shirley background was used for the peak fitting procedure.

3 Results and discussion

3.1 Effect of maximum oxidation potential on growth and crystallization of titanium anodized films

The AFM images and their cross sections of anodic oxide films on sputter-deposited titanium formed under CV mode with the potential sweep rate of 0.1 mV/s for different φ_{max} are displayed in Fig. 1. For the oxide film grown with low φ_{max} (200 mV), the film surface is relatively flat, and few grains can be seen (Fig. 1(a)). While for the φ_{max} of 1000 mV, numerous of individual grains with an average diameter of about 100 nm emerge on the sample surface (Fig. 1(b)). Subsequently, when the φ_{max} is set as 2000 mV, the shape of the grains is much clearer, and the grains in size (about 130 nm) are almost uniform throughout the film surface (Fig. 1(c)). As revealed in the literature, these nanoscale grains formed on titanium anodized films surface are considered to be mainly composed of anatase

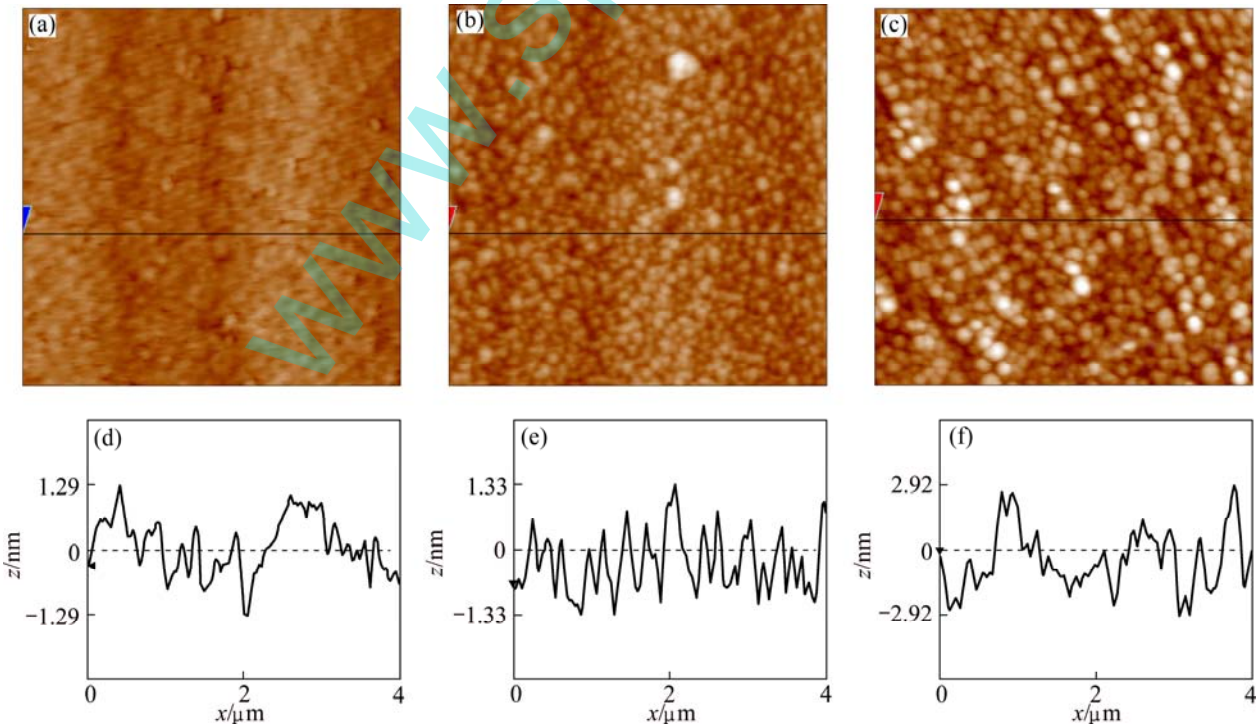

Fig. 1 AFM images (a, b, c) and their cross sections (d, e, f) of titanium oxide films obtained by CV mode with potential sweep rate of 0.1 mV/s and φ_{max} of 200 mV (a, d), 1000 mV (b, e) and 2000 mV (c, f)

nanocrystals [12]. That is to say, high applied voltages are beneficial for the generation of crystalline titanium oxides.

Figure 2 presents the influence of φ_{max} on the surface roughness and thickness of titanium oxide films under CV mode. As seen in the diagram, the R_a and R_{ms} of the anodized samples increase gradually with applied potentials increasing, which could be a result of the formation of anatase crystalline grains. Similar to the surface roughness, the thickness of titanium anodized films also shows a growing tendency as the φ_{max} increases, with a growth rate of about 3 nm/V.

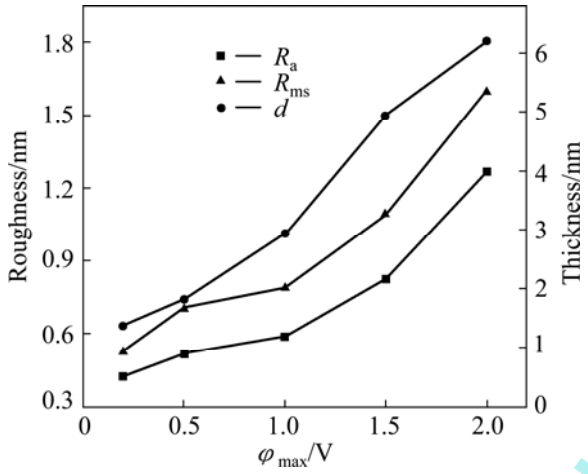

Fig. 2 Surface roughness (R_a and R_{ms}) and film thickness (d) of titanium oxide films formed under CV mode with potential scanning rate of 0.1 mV/s at different φ_{max}

The optical properties, including the refractive index (n) and extinction coefficient (k), of titanium oxide film obtained under CV mode with the φ_{max} of 1500 mV and the potential sweep rate of 0.1 mV/s are shown in Fig. 3. The n and k are seen to increase with the wavelength. As reported in Ref. [12], the n value is determined by the structure of titanium oxide films on very smooth titanium samples. At the wavelength of 632.8 nm, the n value is reported as 2.2 for amorphous titanium oxides, while for anatase TiO_2, n is about 2.55 [17]. As shown in Fig. 3, the n value of the grown film at 632.8 nm is 2.357, which is higher than that of the amorphous film but lower than that of the anatase titanium oxide, indicating that the film is composed of anatase and amorphous structure. If the content of the amorphous oxide is set as x, the crystallinity of the anodized film can be calculated by the following equation [12]:

$$n_{film}= n_{amorphous}x+n_{anatase}(1-x)$$

The n value at 632.8 nm and the crystallinity of titanium anodized film formed by CV mode with the potential sweep rate of 0.1 mV/s for different φ_{max} are summarized in Table 1. As shown in Table 1, the crystallinity of titanium oxide films increases with φ_{max}, which is in good agreement with the AFM results shown in Fig. 1. For the film formed at a very low potential (200 mV), the structure of titanium oxide is amorphous. By contrast, for the film grown at 2000 mV, the content of the anatase increases up to 68%.

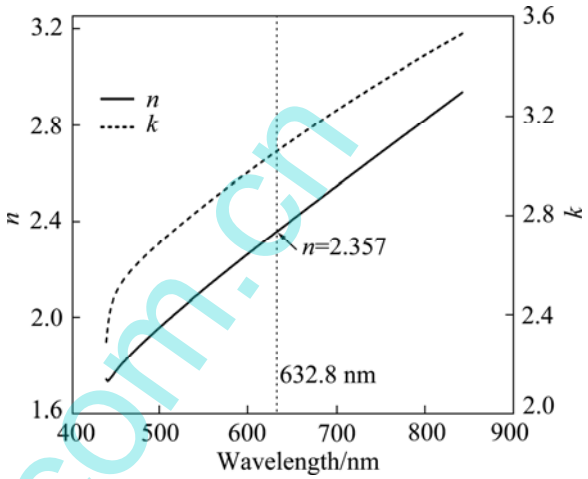

Fig. 3 Optical properties of titanium oxide film formed under CV mode with potential scanning rate of 0.1 mV/s and φ_{max} of 1500 mV

Table 1 Refractive index at wavelength of 632.8 nm and crystallization degree of titanium oxide films formed under CV mode with potential sweep rate of 0.1 mV/s and different φ_{max}

φ_{max}/mV	n	Crystallinity/%	
		Amorphous	Anatase
200	2.198	100	0
500	2.207	98	2
1000	2.258	83.43	16.57
1500	2.357	55.14	44.86
2000	2.438	32	68

For the anodic oxide film on sputter-deposited titanium grown at very low potential (φ_{max}=1000 mV), as shown in Fig. 4(a), the Ti 2p XPS spectra can be resolved into 6 peaks, corresponding to Ti^{2+}, Ti^{3+} and Ti^{4+}, respectively. This implies that the oxide films formed at low potentials are mainly composed of TiO_2, and also contain some titanium suboxides. The O 1s XPS spectrum recorded from the anodized sample surface can be fitted with 3 peaks, which are attributed to O^{2-}, OH^- and H_2O, respectively (Fig. 4(b)). As mentioned by some investigators, the O^{2-} species is from TiO_2, and the OH^- and H_2O are acted as bound water or absorbed water in the film [18,19].

Figure 5 presents the evolution of the contents of O^{2-}, OH^-, H_2O (for O element), Ti^{4+}, Ti^{2+} and Ti^{3+} (for Ti

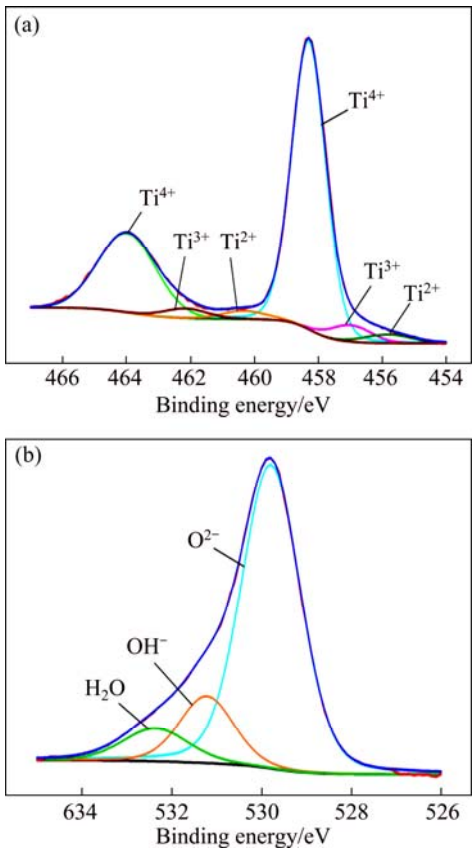

Fig. 4 Ti 2p (a) and O 1s (b) XPS spectra of titanium oxide film obtained under CV mode with potential scanning rate of 0.1 mV/s and φ_{max} of 1000 mV

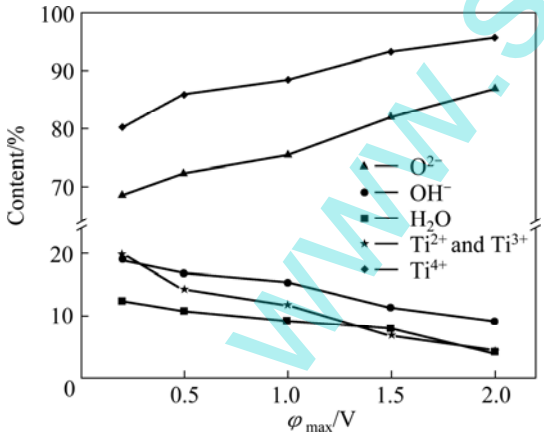

Fig. 5 Contents of O^{2-}, OH^-, H_2O (for O element), Ti^{4+}, Ti^{2+} and Ti^{3+} (for Ti element) of titanium oxide films as a function of φ_{max} (potential sweep rate is 0.1 mV/s)

element) of titanium anodized films with φ_{max} under CV mode. It is clearly shown that the O^{2-} and Ti^{4+} species increase while the OH^-, H_2O, Ti^{2+} and Ti^{3+} species decrease gradually with φ_{max} increasing. This implies that high applied voltages are beneficial for the generation of TiO_2 and for the dehydration process during titanium anodization. In addition, as mentioned in Ref. [13,20], the titanium suboxides and the bound water are considered to be the disorder source in anodic oxide films. Therefore, it can be concluded from the XPS results (Fig. 5) that high applied potentials are good for the crystallization of titanium anodized films.

3.2 Effect of potential sweep rate on growth and crystallization of titanium anodized films

Figure 6 displays the AFM images and their cross sections of titanium anodized films which are formed under CV mode with the same φ_{max} (1000 mV) and different potential scanning rates. The AFM image of the film grown at 1000 mV with the potential sweep rate of 0.1 mV/s is shown in Fig. 1(b). Comparing the surface topography of titanium oxide films formed with different potential scanning rates, it can be found that the anatase grains turn to clearer and sharper as the potential sweep rate decreases. Moreover, as can be seen in Fig. 7, the surface roughness (R_a and R_{ms}) and thickness are higher for the oxide films formed with lower potential scanning rate. These findings may imply that lower potential sweep rate (or longer anodizing time) is beneficial for the growth and crystallization of titanium oxide films.

Table 2 summarizes the n value at 632.8 nm and the crystallinity of titanium anodized films grown at CV mode with φ_{max} of 1000 mV for different potential scanning rates, the n value and the content of anatase for the film formed at 1000 mV with the potential sweep rate of 0.1 mV/s can be found in Table 1. It is clear that the crystallinity of titanium oxide film increases with decreasing potential scanning rate. This means that the film crystallization is encouraged by reducing the potential sweep rate, which is in good agreement with the AFM results.

The contents of O^{2-}, OH^-, H_2O (for O element), Ti^{4+}, Ti^{2+} and Ti^{3+} (for Ti element) of the anodized samples formed at 1000 mV with different potential scanning rate are shown in Fig. 8. As shown in the figure, the O^{2-} and Ti^{4+} species decrease while the OH^-, H_2O, Ti^{2+} and Ti^{3+} species increase progressively with the increase of the potential sweep rate. That is to say, reducing the potential scanning rate is beneficial for the generation of dehydrated and TiO_2 dominated titanium anodized films, and then facilitating the film growth and crystallization.

3.3 Growth and crystallization of titanium oxide films at very low potentials

The φ—J curves of the fifth CV cycle of titanium anodization with different φ_{max} for the potential scanning rate of 0.1 mV/s are presented in Fig. 9. At the beginning of each CV cycle, an active-passive transition (J_c) of the film can be seen [21]. The value of J_c increases with φ_{max}, especially for φ_{max} of 1500 mV. Subsequently, the current

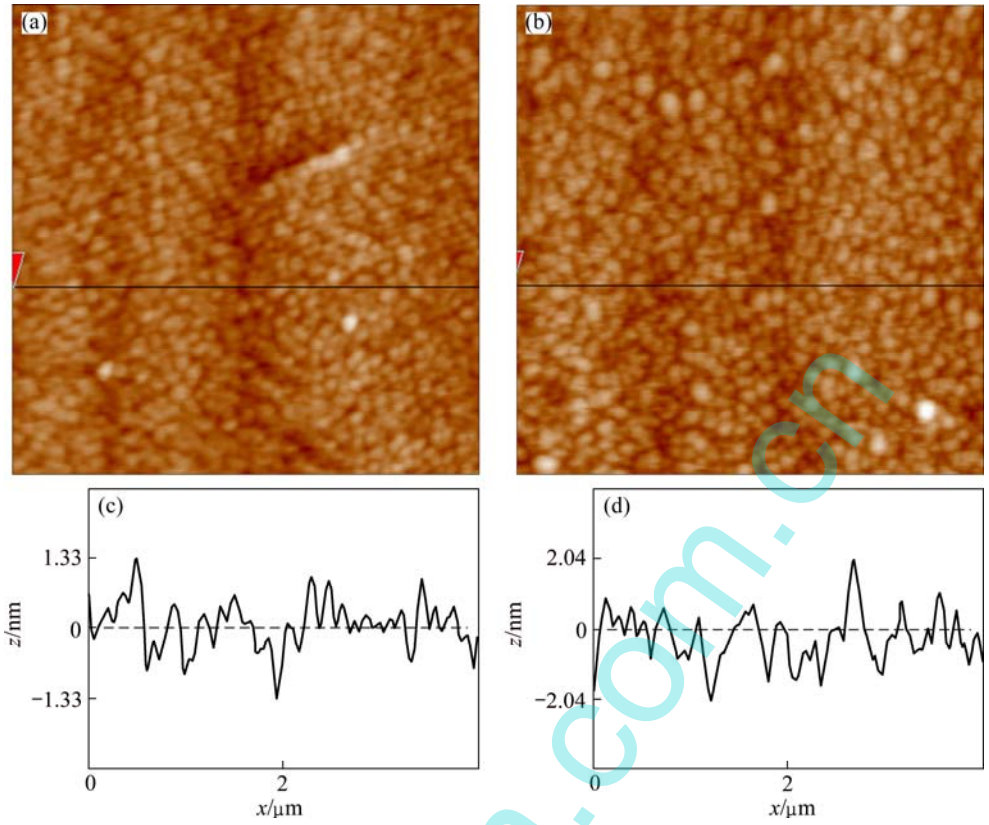

Fig. 6 AFM images (a, b) and their cross sections (c, d) of titanium oxide films obtained by CV mode with φ_{max} of 1000 mV and potential sweep rate of 0.5 mV/s (a, c) and 0.05 mV/s (b, d)

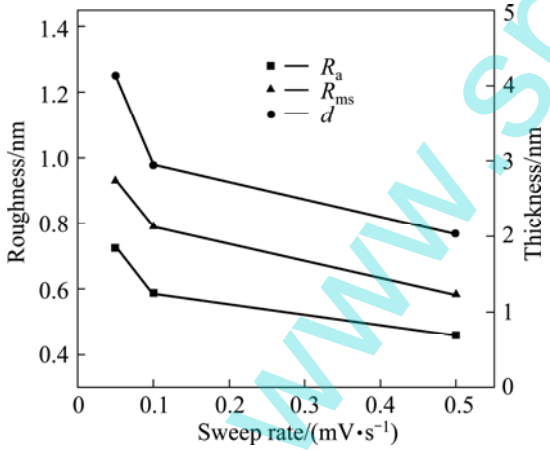

Fig. 7 Surface roughness (R_a and R_{ms}) and film thickness (d) of titanium anodized films grown under CV mode with φ_{max} of 1000 mV at different potential sweep rates

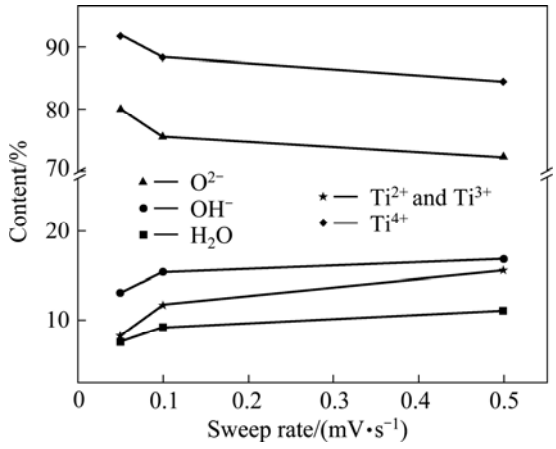

Fig. 8 Contents of O^{2-}, OH^-, H_2O (for O element), Ti^{4+}, Ti^{2+} and Ti^{3+} (for Ti element) of titanium anodized films obtained under CV control with φ_{max} of 1000 mV for different potential sweep rates

Table 2 Refractive index at wavelength of 632.8 nm and crystallinity of titanium oxide films formed under CV mode with φ_{max} of 1000 mV at different potential sweep rates

Sweep rate/ ($mV \cdot s^{-1}$)	n	Crystallinity/%	
		Amorphous	Anatase
0.05	2.293	73.43	26.57
0.5	2.241	88.29	11.71

density stays at about zero and turns to be negative at the end of the CV cycle. This means that the film formation and film dissolution performed alternately during each CV cycle of titanium anodization. Moreover, for the titanium anodizing with the φ_{max} of 1500 mV, there is also a current density (J_o) increase at about 1200 mV due to the occurrence of oxygen evolution. The oxygen evolution is considered to be favorable for the growth

and crystallization of titanium anodized films [16,22]. This could be the main reason why the thickness and the crystallinity of the formed films have a sudden increase for the φ_{max} of 1500 mV (as shown in Fig. 2 and Table 1).

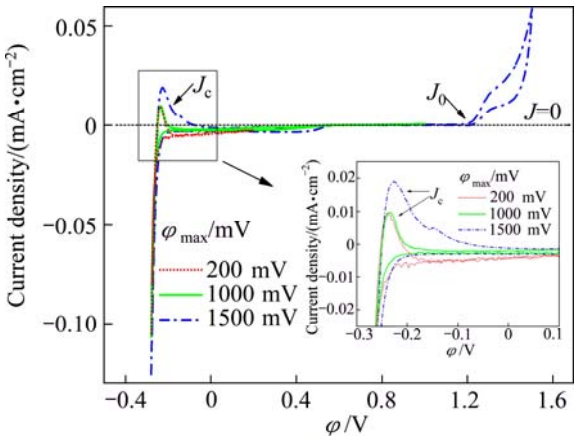

Fig. 9 φ—J curves of titanium oxide film obtained under CV mode with different φ_{max} for potential sweep rate of 0.1 mV/s

Most of the researchers agreed that the crystallization of anodic titanium oxide films was mainly encouraged by the local joule heating, and the crystalline titanium oxides would be formed only when the applied current density (or the applied potential) was high enough [23,24]. While in our present study, the oxide films formed at very low potentials (as low as 1000 mV) clearly show a crystalline behavior, and both enlarging the applied potentials and reducing the potential sweep rate facilitate the film crystallization (see Table 1 and Table 2). That is to say, the crystallization of titanium anodized films at very low potentials must be due to other reasons, such as the internal compressive stress generated in the film [18,25].

The transition of amorphous films into crystalline ones will be encouraged by the compressive stress in the film for the reason that the former usually occupies larger volume than the later [26,27]. As mentioned in Ref. [25], for titanium anodization, the volume of the oxide formed is much larger compared with the metal consumed, hence large compressive stress will be produced as a result of the titanium oxides growth at the oxide/metal interface. In this work, the film growth goes through a very slow process, and titanium oxides dissolve and re-form alternately, which is beneficial for the generation of internal compress stress. Moreover, as revealed by SE, enhancing the applied voltages or reducing the potential sweep rate promotes the growth of titanium oxide films (see Fig. 2 and Fig. 7), so that more compressive stress will be produced at the oxide/metal interface, and as a result, the crystallization of titanium anodized films is encouraged.

4 Conclusions

The anodizing of the sputter-deposited titanium samples is performed at CV mode in sulfuric solution at very low potentials, and the effect of the applied potentials and the potential scanning rate on the surface topography, crystallization and chemical composition of the formed oxide films are studied. The results show that the films grown with higher φ_{max} or with lower potential sweep rate are rougher, thicker and more crystalline. Enlarging the φ_{max} or reducing the potential scanning rate is also proved to be beneficial for the growth of dehydrated and TiO_2 dominated anodic oxide films.

References

[1] KHAMENEH ASL S, ALAVI B, AHMADI S. The effect of highly ordered titania nanotube structures on hydrogen gas detection [J]. Surface and Interface Analysis, 2012, 44(8): 1051−1053.

[2] DUBEY M, HE H. Effect of titanium substrate morphology on the growth of TiO_2 nanotubes and their photovoltaic performance in dye-sensitized solar cells [J]. Nanoscience and Nanotechnology Letters, 2012, 4(5): 548−552.

[3] DIAMANTI M, ORMELLESE M, MARIN E, LANZUTTI A, MELE A, PEDEFERRI M. Anodic titanium oxide as immobilized photocatalyst in UV or visible light devices [J]. Journal of Hazardous Materials, 2011, 186: 2103−2109.

[4] MANTZILA A G, PRODROMIDIS M I. Development and study of anodic Ti/TiO_2 electrodes and their potential use as impedimetric immunosensors [J]. Electrochimica Acta, 2006, 51(17): 3537−3542.

[5] ZOU Jian-peng, WANG Ri-zhi. Crack initiation, propagation and saturation of TiO_2 nanotube film [J]. Transactions of Nonferrous Metals Society of China, 2012, 22(3): 627−633.

[6] TANG Yu-xin, TAO Jie, ZHANG Yan-yan, WU Tao, TAO Hai-jun, ZHU Ya-yong. Preparation of TiO_2 nanotube on glass by anodization of Ti films at room temperature [J]. Transactions of Nonferrous Metals Society of China, 2009, 19(1): 192−198.

[7] HENDERSON M A. A surface science perspective on TiO_2 photocatalysis [J]. Surface Science Reports, 2011, 66(6−7): 185−297.

[8] MASAHASHI N, MIZUKOSHI Y, SEMBOSHI S, OHTSU N. Enhanced photocatalytic activity of rutile TiO_2 prepared by anodic oxidation in a high concentration sulfuric acid electrolyte [J]. Applied Catalysis B, 2009, 90(1−2): 255−261.

[9] LEE B G, CHOI J W, LEE S E, JEONG Y S, OH H J, CHI C S. Formation behavior of anodic TiO_2 nanotubes in fluoride containing electrolytes [J]. Transactions of Nonferrous Metals Society of China, 2009, 19(4): 842−845.

[10] SI H, SUN Z, KANG X, ZI W, ZHANG H. Voltage-dependent morphology, wettability and photocurrent response of anodic porous titanium dioxide films [J]. Microporous and Mesoporous Materials, 2009, 119: 75−81.

[11] OHTSUKA T, GUO J, SATO N. Raman spectra of the anodic oxide film on titanium in acidic sulfate and neutral phosphate solutions [J]. Journal of the Electrochemical Society, 1986, 133: 2473−2476.

[12] XIA Z, NANJO H, TETSUKA H, EBINA T, IZUMISAWA M, FUJIMURA M, ONAGAWA J. Crystallization of the anodic oxide on titanium in sulphuric acids solution at a very low potential [J]. Electrochemistry Communications, 2007, 9(4): 850−856.

[13] XIA Z, NANJO H, AIZAWA T, KANAKUBO M, FUJIMURA M, ONAGAWA J. Growth process of atomically flat anodic films on

titanium under potentiostatical electrochemical treatment in H_2SO_4 solution [J]. Surface Science, 2007, 601(22): 5133−5141.
[14] da FONSECA C, TRAVERSE A, TADJEDDINE A, BELO M D C. A characterization of titanium anodic oxides by X-ray absorption spectroscopy and grazing X-ray diffraction [J]. Journal of Electroanalytical Chemistry, 1995, 388(1−2): 115−122.
[15] MARSH J, GORSE D. A photoelectrochemical and ac impedance study of anodic titanium oxide films [J]. Electrochimica Acta, 1998, 43(7): 659−670.
[16] HABAZAKI H, UOZUMI M, KONNO H, SHIMIZU K, SKELDON P, THOMPSON G. Crystallization of anodic titania on titanium and its alloys [J]. Corrosion Science, 2003, 45(9): 2063−2073.
[17] MICHAELIS A, DELPLANCKE J, SCHULTZE J. Ellipsometric determination of the density of TiO_2 passive films on Ti single crystals: Combination of ellipsometry and coulometry [C]//Materials Science Forum. Switzerland: Trans Tech Publ, 1995: 471−480.
[18] SHIBATA T, ZHU Y. The effect of film formation conditions on the structure and composition of anodic oxide films on titanium [J]. Corrosion Science, 1995, 37: 253−270.
[19] OHTSUKA T. The aging of the anodic oxide of titanium during potentiostatic condition by ellipsometry [J]. Corrosion Science, 2003, 45: 1793−1801.
[20] OHTSUKA T, NOMURA N. The dependence of the optical property of Ti anodic oxide film on its growth rate by ellipsometry [J]. Corrosion Science, 1997, 39: 1253−1263.
[21] SHIBATA T, ZHU Y. The effect of temperature on the growth of anodic oxide film on titanium [J]. Corrosion Science, 1995, 37: 133−144.
[22] MATYKINA E, ARRABAL R, SKELDON P, THOMPSON G, HABAZAKI H. Influence of grain orientation on oxygen generation in anodic titania [J]. Thin Solid Films, 2008, 516(8): 2296−2305.
[23] VANHUMBEECK J, RYELANDT L, PROOST J. On the relationship between local voltage maxima and efficiency changes during galvanostatic Ti anodising [J]. Electrochimica Acta, 2009, 54: 3330−3338.
[24] YAHALOM J, ZAHAVI J. Electrolytic breakdown crystallization of anodic oxide films on A1, Ta and Ti [J]. Electrochimica Acta, 1970, 15: 1429−1435.
[25] NELSON J, ORIANI R. Stress generation during anodic oxidation of titanium and aluminum [J]. Corrosion Science, 1993, 34: 307−326.
[26] LEACH J, PEARSON B. Crystallization in anodic oxide films [J]. Corrosion Science, 1988, 28: 43−56.
[27] PILLING N, BEDWORTH R. The oxidation of metals at high temperatures [J]. J Inst Metals, 1923, 29: 529−582.

极低电位下溅射沉积钛表面阳极氧化膜的生长与结晶

邢俊恒，夏正斌，李 辉，王莹莹，钟 理

华南理工大学 化学与化工学院，广州 510640

摘 要：以磁控溅射法沉积在单晶硅片上的钛薄膜样品为工作电极，以循环伏安法为阳极氧化方式，研究极低电位下钛表面氧化膜的生长与结晶行为。通过 AFM、SE 和 XPS 等手段表征钛表面阳极氧化膜的表面形貌、结晶性和化学组成。结果表明，即使在低至 1000 mV 的电位下，所形成的阳极氧化钛薄膜也是结晶的，而不是无定型的。升高氧化电位或者降低电位扫描速率都有利于钛氧化膜的形成和结晶。认为，在极低的电位下，产生于氧化膜/金属界面的内在压应力是导致钛氧化物结晶形成的主要原因，而不是被研究者们所普遍接受的焦耳热。

关键词：阳极氧化；溅射沉积钛；结晶；低电位；循环伏安法

(Edited by Hua YANG)